PAPER

Optical Node Architectures That Utilize Dedicated Add/Drop Switches to Realize Colorless, Directionless and Contentionless Capability

Yoshiyuki YAMADA[†a)], ***Student Member***, **Hiroshi HASEGAWA**[†], ***Senior Member***, ***and*** **Ken-ichi SATO**[†], ***Fellow***

SUMMARY This paper proposes optical node architectures for the single-layer optical cross-connect (OXC) and hierarchical OXC (HOXC) that utilize dedicated add/drop switches for originating/terminating traffic at a node. For both single-layer OXC and HOXC, three architectures with different restrictions on add/drop capabilities are presented. The performance of the proposed architectures is compared through numerical experiments. The architectures significantly reduce total switch scale and minimize necessary switch size while attaining colorless, directionless and contentionless capabilities.

key words: *optical cross-connect, colorless/directionless/contentionless, waveband, multi-layer optical paths*

1. Introduction

The continual increase in traffic volume is driving the penetration of single-layer optical path network technologies due to their cost effectiveness and low power consumption [1], [2]. In the single-layer optical path network, optical paths are switched at the granularity level of the wavelength path by using the optical cross-connect (OXC). New video-centric broadband services including ultra-high definition TV are advancing [3]. E-science is also another of the cutting-edge applications [4]. The result will be an explosion in traffic volume in the near future.

To cope with this traffic expansion, the hierarchical optical path network has been investigated [5]–[9]. The hierarchical OXC (HOXC) introduces the waveband path (a bundle of multiple wavelength paths) as a higher-order optical path. The HOXC consists of waveband cross-connect (WBXC) and wavelength cross-connect (WXC) [5]–[9]. It has been verified that a hierarchical optical path network with waveband routing can greatly reduce the total number of optical switch ports [5]–[7]. The work in [10] clarified the direct relationship of the port count reduction achieved by the hierarchical optical path network to the average hop number of waveband paths and the average waveband utilization. These parameter values strongly depend on the performance of the network design algorithm used. Efficient heuristic algorithms have been developed [11], [12] that can reduce total network cost, i.e. necessary port count and the number of fibers in the network. The algorithm proposed in [12] utilizes an efficient strategy to group closely located wavelength paths. Other algorithms [13], [14] focus on network survivability, that is, network design that considers protection mechanisms in the waveband path layer [13] and in the wavelength path layer [14], respectively. Another work, [15], addressed the design problem by setting waveband add/drop ratio constraints because the ratio should be minimized in order to reduce necessary switch size. The waveband add/drop ratio is the ratio of the number of added/dropped waveband paths to that of all outgoing/incoming waveband paths. [15] suggests that combining an appropriate HOXC architecture with tailored network design that can control the waveband add/drop ratio makes it possible to optimize the scale of switch hardware and the total network cost.

Several studies provided HOXC node architectures and detailed analyses [16]–[18]. The substantial effectiveness of the HOXCs in terms of switch scale has been confirmed. This was verified for both the matrix switch based HOXC [16], [17], and the wavelength/waveband selective switch based HOXC [18]. In fact, an ultra-compact WBXC module that yields good transmission performance has been developed recently [19]. These studies clarified that the reduction in switch size strongly depends on the waveband add/drop ratio because the WXC is the dominant part of the HOXC. Although the proposed HOXC architectures can reduce switch size, further switch scale reduction is still needed. We have already proposed an HOXC architecture that separately handles two categories of add/drop wavebands; those that are originated/terminated and those that are groomed [20]. The architecture can reduce the total switch size since added/dropped wavelength paths from/to the electrical layer do not need to pass through the WXC part.

An OXC with colorless, directionless and contentionless (C/D/C) capability is the key to creating flexible optical networks [21], [22]. These capabilities are of critical importance in configuring optical paths to respond to continually changing network situations quickly and economically without manual operations. A transponder is colorless if it can connect any wavelength channel to any fiber port, which can be done with a tunable transponder. Directionless operation enables each transponder to access any input/output fiber. The contentionless functionality allows multiple transpon-

Manuscript received May 9, 2011.
Manuscript revised November 15, 2011.

[†]The authors are with the Department of Electrical Engineering and Computer Science, Nagoya University, Nagoya-shi, 464-8603 Japan.
a) E-mail: yo_yamad@echo.nuee.nagoya-u.ac.jp

DOI: 10.1587/transcom.E95.B.1307

ders to access different fibers simultaneously with the same wavelength. Usually the switch scale necessary for implementing the C/D/C function is very large and costly. For example, to handle 8 optical fibers, each carrying 96 wavelength channels, the OXC needs a huge 768×768 switch just for C/D/C operation, which is obviously impractical. It is therefore natural to limit the maximum number of wavelength paths that can be originated or terminated at the OXC, since only a portion of the paths, say 20–50%, are terminated/originated at each node. Recently, some studies proposed optical node architectures targeting C/D/C capability [23], [24]. The ROADM architecture shown in [23] lacks flexibility because the ROADM limits the number of input/output signals by bank units, i.e. fiber granularity. The C/D/C architecture presented in [24] decreases the C/D/C switch size by dividing the C/D/C part into two stages. However, its switch scale reduction is limited because a large number of wavelength paths at the C/D/C switch part, that is, a large number of input switch ports for the drop side C/D/C switch and a large number of output ports for the add side C/D/C switch, are required for C/D/C matrix switches.

In this paper, we propose novel matrix-switch-based optical node architectures that are applicable for the single-layer OXC and HOXC that can reduce C/D/C switch scale. The reason for adopting the matrix type is that actual switch components are now available, and in addition, the hardware implementation of an 8×8 large capacity HOXC system with $80\,\lambda$ channels per fiber has been reported [25]. The development of large scale matrix switches based on silicon photonics has been extensively studied, and as a result, the matrix switch technology is advancing rapidly. Considering these facts, this paper focuses on matrix switch based systems. The proposed node architecture employs dedicated add/drop switches with through ports for originating/terminating optical paths. We can also apply wavelength/waveband selective switch (WSS/WBSS) to the dedicated switch portion as well as the cross-connect portion. WSS (WBSS) can transport arbitrary combinations of wavelength (waveband) paths to a relatively small number of output ports, in other words, each output port is densely used, which is a good point of WSS/WBSS. In drop operation, however, it is required to deliver a single wavelength (waveband) path to each output port of WSS/WBSS. Each output port is used by a single wavelength (waveband) path, which means the property of WSS/WBSS does not always suit the drop operation. To realize the same functions as the proposed architectures, a lot of WSS/WBSSs or significantly high degree WSS/WBSSs are necessary. In addition to the WSS/WBSS, space switches will be necessary to attain contentionless capability. Therefore, we consider here matrix switches that suit drop functions. The introduction of dedicated switches enables minimization of the number of inputs/outputs at the C/D/C switch part, which can reduce the C/D/C switch size. Furthermore, in the proposed HOXC node, the introduction of dedicated add/drop switches also leads to a decrease in the size of the WXC part. The configuration of the C/D/C switch itself is not discussed herein. The same switches are necessary to realize the C/D/C functionality for both single-layer OXC and HOXC. The switches for the cross-connect through part need to be optic because transparent transmission is desirable. Regarding the C/D/C switching part, however, we have other options to handle the paths in relation to intra-office transmission; namely, we can deploy the C/D/C switch after terminating the optical paths. In that situation, the C/D/C switches are not necessarily optical switches. Several technologies for creating the C/D/C switch are known, for example, optical or electrical space switches or using ODU cross-connects if sub-λ granularity is also necessary. Starting from our previous work, which introduced a node architecture with dedicated add/drop functionality, this paper, for the first time, offers a strategy to effectively reduce C/D/C switch scale. First, we summarize the conventional switch architectures and the main concept of the proposed switch architecture. Several architectures are then proposed considering different add/drop restrictions. A quantitative analysis shows that the proposed node architectures can substantially reduce total switch scale.

2. Preliminaries

2.1 Conventional Switch Architectures for Single-Layer OXC and HOXC

Figures 1 and 2 depict conventional switch (SW) architectures for the single-layer OXC and HOXC, respectively. Let K be the number of input or output fibers and L the number of wavelength paths per fiber. The originating/terminating ratio, the ratio of the number of optical paths for termination or origination to that of all incoming/outgoing optical paths, is denoted as z. The conventional single-layer OXC has L $(1 + z)K \times (1 + z)K$ matrix SWs for each group of optical paths with the same wavelength index, see Fig. 1 [16]. This architecture imposes a limit on the number of originated/terminated wavelength paths within each wavelength index group. For the HOXC, let M be the number of waveband paths per fiber, N the number of wave-

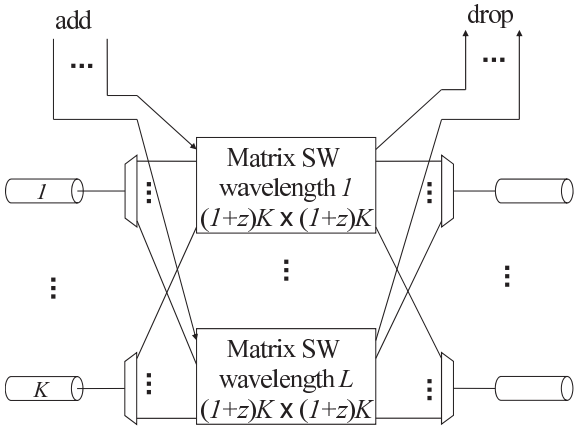

Fig. 1 Conventional single-layer OXC.

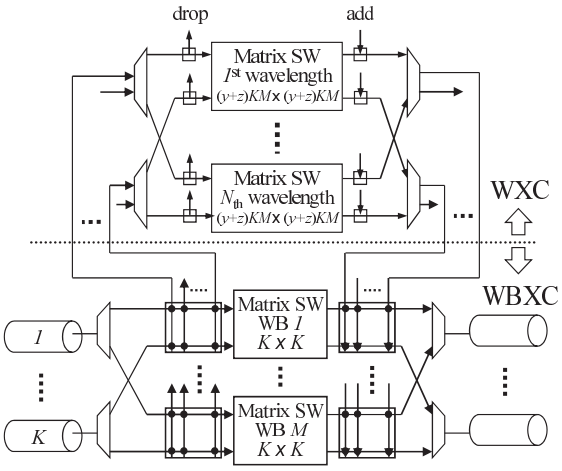

Fig. 2 Conventional HOXC architecture.

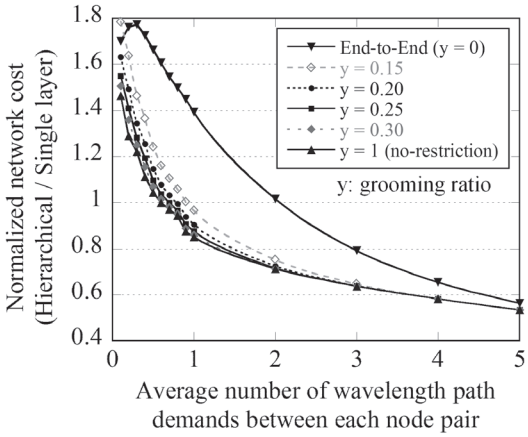

Fig. 3 Normalized network cost for 9×9 regular mesh network ($M = 8$, $N = 12$).

length paths per waveband, and y the grooming ratio; the grooming ratio means the ratio of the number of waveband paths that can be reconfigured at the WXC part to that of all incoming/outgoing waveband paths. The conventional HOXC has M $K \times K$ matrix SWs for each waveband index group, and N $(y + z)KM \times (y + z)KM$ matrix SWs for each i-th wavelength index in incoming wavebands. In addition, this HOXC uses $2K$ matrix SWs specially designed for waveband add/drop operations and colorless wavelength multi/demultiplexers (MUXs/DEMUXs) that can be commonly used by any waveband index so as to achieve colorless waveband add/drop operation. For more details of this configuration, refer to [17]. In the node architecture proposed in this paper, we assume that these SW architectures are used as the cross-connect part denoted as the single-layer OXC or HOXC, except for the add/drop functional parts from/to the electrical layer, since they are one of the most advanced matrix-switch based architectures in single-layer and hierarchical cross-connect nodes [16], [17].

2.2 Concept of Proposed Node Architectures with Dedicated Add/Drop Switch for Termination

The basic concept of our proposal is splitting the add/drop functions into those for originating/terminating waveband paths and those for grooming waveband paths. The corresponding ratios are called the originating/terminating ratio and the grooming ratio. In a previous study [20], we proposed a preliminary version of a new HOXC architecture. This concept can be straightforwardly applied to conventional single-layer OXCs (replace HOXC with single-layer OXC). The important point is that it is possible to employ small SWs dedicated to specific functions. The minimal number of ports needed for the C/D/C part is determined by the traffic demands from the upper layer, i.e. the electrical layer. Therefore, the proposed separate architecture can make the required originating/terminating ratio independent of the number of input/output fibers at the node. It should be noted that we can control only the number of grooming optical paths, and not the number of terminating wavelength paths.

We have proposed a static network design algorithm that is applicable to our proposed HOXC architecture [20]. The proposed algorithm makes the best use of coarse granular routing while limiting fine granular grooming by setting the grooming ratio bound. Figure 3 shows the simulation results for our proposed algorithm under the condition of $M = 8$, $N = 12$, and a 9×9 regular mesh network. The grooming ratio y is upper-bounded by each represented value. The network costs are normalized by those of the equivalent single layer optical path network. As shown in Fig. 3, our proposed design algorithm can achieve significant network cost reductions. Even when the grooming ratio is restricted to 0.20, the proposed algorithm provides almost the same network costs as that with no restriction for all traffic demand areas. This means that the HOXC offers substantial switch scale reduction compared to the single-layer OXC in the cross-connect part; about 50% reduction can be attained for the matrix switch based case with parameters of $K = 8$, $M = 8$, $N = 12$. This evaluation is calculated by the formulations shown in the table of paper [13].

In this paper, the grooming ratio is set to be 0.25. The important point to be noted is that the carriers do not need to care about the optimal value of the grooming ratio. What the carriers should do is to declare the amount of originating or terminating traffic (number of wavelength paths) at each node and node degree. With these values, the network design algorithm automatically determines necessary switch hardware scale to accommodate the given demands with consideration of the grooming ratio restriction.

3. Proposed Node Architectures

Figure 4 depicts the functional diagram of proposed node architectures. At the first stage, a dedicated SW for termination, incoming optical signals are separated into those terminated at the node and those forwarded to other nodes. The second stage provides the cross-connect function. The

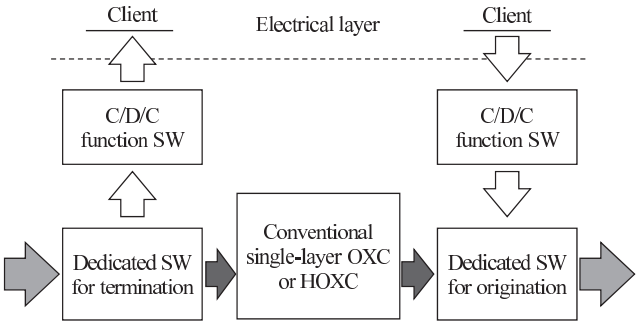

Fig. 4 Overall structure of proposed node architecture.

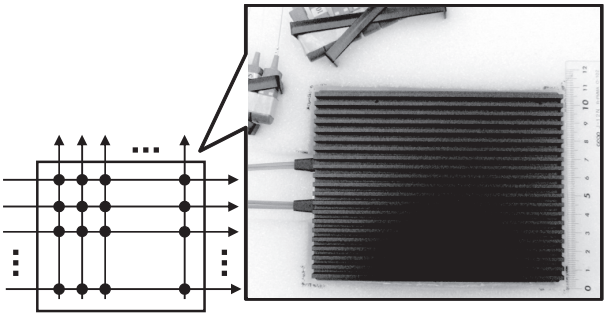

Fig. 5 Developed 16 × 16 matrix switch with 16 through ports.

optical paths are routed with wavelength path granularity or waveband path granularity by using conventional single-layer OXC or HOXC, respectively. The dedicated SW for origination traffic at the third stage transmits the optical paths to adjacent nodes by merging optical paths from the cross-connect part and optical paths originated at the node. Discussion in this paper is focused on just the drop side of the node, that is, the drop side SW for termination. The same SW architecture can be applied to the add side SW for origination paths by reversing the optical signal direction.

3.1 Single-Layer OXC Architectures Considering Three Kinds of Originating/Terminating Ratios

We propose three single-layer OXC architectures that impose different drop restrictions. Dedicated drop SW part can be realized by the matrix SWs that have through ports used in conventional HOXC nodes. We have already developed 16 × 16 matrix SWs with 16 through ports and good performance was confirmed (Fig. 5) [17].

Figure 6(a) shows a single-layer OXC that restricts the wavelength terminating ratio; this ratio is unrelated to fiber or wavelength index. We call this restriction the total restriction (TR). To implement the total restriction, this architecture consists of $K \times K$ matrix SWs that have through ports, star couplers and $1 \times L$ SWs. The number of $K \times K$ matrix SWs, L, equals the number of wavelength paths per fiber. The branch number of the star coupler and the number of $1 \times L$ SW is determined by the number of fibers, K, and terminating ratio z. Thus, the number of ports of each star coupler is zL and the number of $1 \times L$ switches is zKL. In

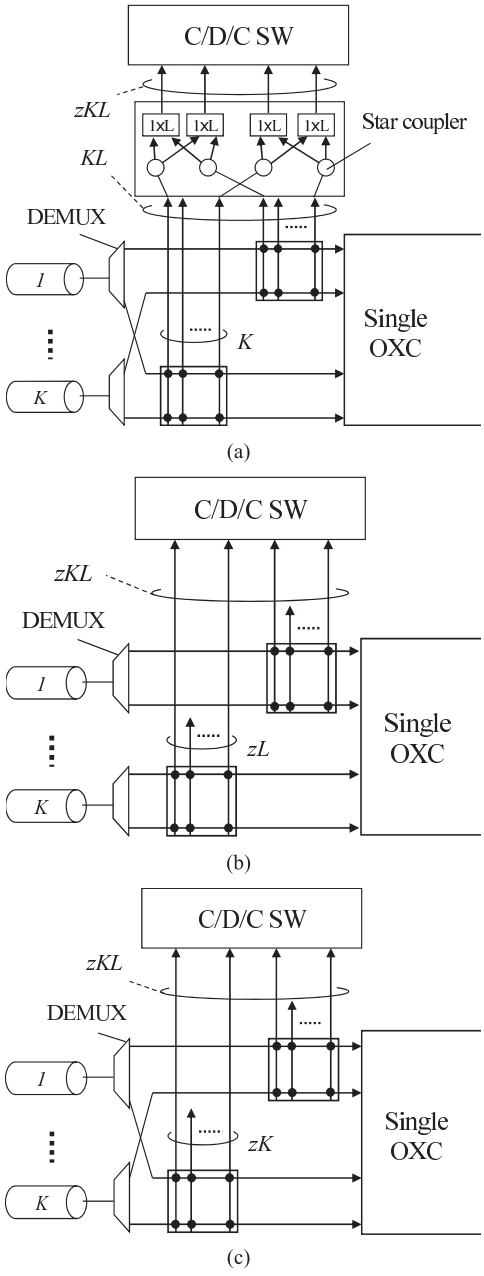

Fig. 6 Proposed single-layer OXC architectures with restriction on the wavelength terminating ratio (only drop part is illustrated). (a) total restriction (TR). (b) each fiber restriction (EFR). (c) each wavelength restriction (EWR).

this TR architecture, the components combined with these star couplers and $1 \times L$ switches provides the dropping function where the number of terminating wavelength paths is restricted to zKL irrespective of input fiber or wavelength channel. If these components are not used, the $K \times K$ matrix switches with through ports are allocated for each wavelength index, that is, the structure is the same as in the EWR architecture with $z = 1.0$. The module consisting of the star couplers and $1 \times L$ switches is the key point of the proposed TR architecture.

Figure 6(b) displays a single-layer OXC that limits the

Table 1 Comparison of proposed single-layer OXC architectures.

Kinds of restriction	Figure	SW element	# of SC	# of cross-points
Total - TR	Fig. 6(a)	$K \times K$	KL	$2K^2L + 2zKL(L-1) + K^2L$
Each fiber - EFR	Fig. 6(b)	$L \times zL$	-	$2zKL^2 + K^2L$
Each wavelength - EWR	Fig. 6(c)	$K \times zK$	-	$2zK^2L + K^2L$

ratio of terminating wavelength paths for each fiber. We call this type of restriction each fiber restriction (EFR). The dedicated SW part utilizes $L \times zL$ matrix SWs using through ports, which are assigned to each fiber. The number of matrix SWs, K, equals the number of fibers. At each matrix SW, zL output ports allow this SW to limit the number of input ports to C/D/C SW with regard to each fiber.

Figure 6(c) shows a single-layer OXC that restricts the number of terminating wavelength paths in regard to each wavelength index (called each wavelength restriction or EWR). This architecture uses L, $K \times zK$ matrix SWs with through ports for each wavelength index group. By limiting the output ports of each matrix SW to zK, the number of input ports of C/D/C SW is restricted with regard to each wavelength index.

Table 1 summarizes the three proposed single-layer OXC architectures, required SW elements and the number of star couplers and the switch cross-points. Here the matrix switch scale is evaluated by counting the number of element 2×2 cross-point switches. The number of cross-points shown in Table 1 includes not only the dedicated termination SW part but also the dedicated origination SW part and the cross-connect part. In the proposed TR single-layer OXC, please note that the dedicated SW for termination and origination is rearrangeably non-blocking [26]. In the rearrangably non-blocking SW, it may be necessary to reroute already existing paths to establish new paths. An algorithm will be needed to connect input signals to input ports of C/D/C SW. On the other hand, for the proposed EFR or EWR single-layer OXC, the dedicated SW part is strictly non-blocking [26]. A strictly non-blocking SW can establish a path in any order without affecting existing connections. In the dedicated SW part, the role is just to select any path to be dropped from all incoming paths in any order. This is different from the SWs used in the cross-connect part. The rearranging of dropped paths in any order is done by the C/D/C SW.

3.2 HOXC Architectures Considering Three Kinds of Originating/Terminating Ratios

This subsection presents three HOXC architectures with different restrictions on waveband terminating ratio. Similar to the single-layer OXC, matrix SWs with through ports are utilized in the dedicated drop SW part. In the proposed HOXC architectures, switching operation of the dedicated SW is carried out at the waveband path granularity level. In front of the C/D/C SW, these architectures need DEMUXs that offer colorless operation, that is, demultiplexing any waveband path regardless of its index. For example, the cyclic arrayed waveguide grating (AWG) or the specially designed AWG for colorless operation can be applied as these DEMUXs. The DEMUX modules must offer the function of demultiplexing a waveband path and outputting N component wavelength paths irrespective of the waveband index. Since the value of N is the number of wavelength paths in the waveband path, N is at most 10 or 16. Therefore, this DEMUX needs just a small port number AWG, which allows cost-effective implementation and good performance. Multiple devices have been fabricated on a single PLC chip as is presented in [17].

Figure 7(a) shows a TR-HOXC; it limits the waveband terminating ratio, the number of drop waveband paths to total incoming waveband paths, regardless of fiber or waveband index. To realize the total restriction on the number of dropped waveband paths, the dedicated SW module consists of M, $K \times K$ matrix SWs with through ports, star couplers and $1 \times M$ SWs. The branch number of star coupler and the number of $1 \times M$ SW depends on the number of fibers, K, and terminating ratio z. The branch number of the star coupler is, therefore, zM and the number of $1 \times M$ switch is zKM. Similar to the TR architecture for the single-layer case, the combination of star couplers and $1 \times M$ switches is a key module of the TR-HOXC architecture, since it provides the dropping function with a restriction in the number of waveband paths, irrespective of fiber and/or waveband index.

An EFR-HOXC is presented in Fig. 7(b); it restricts the ratio of terminating waveband paths in terms of each fiber. Similar to the EFR single-layer OXC, this architecture utilizes K, $M \times zM$ matrix SWs with through ports. One matrix switch is allocated to each fiber. Each matrix SW performs the same function as the single-layer OXC to limit the number of C/D/C SW inputs with regard to fiber by reducing the output ports of each dedicated SW to zM.

Figure 7(c) shows an EBR-HOXC; it restricts the number of terminating waveband paths in terms of each waveband index. This configuration has L, $K \times zK$ matrix SWs with through ports for each waveband index group. Only in this case, a fixed DEMUX also can be used. Limiting the output ports of each dedicated matrix SW to zK enables the number of input ports of C/D/C SW to be reduced in terms of each waveband index.

The required matrix SW with through ports, the number of star couplers, and switch cross-points of the three proposed HOXC architectures are summarized in Table 2. The number of switch cross-points in each proposed HOXC includes the dedicated SW for termination and the dedicated SW for origination as well as the cross-connect part denoted as HOXC; it includes WXC and WBXC, and specially de-

Table 2 Comparison of proposed HOXC architectures.

Kinds of restriction	Figure	SW element	# of SC	# of cross-points
Total - TR	Fig. 7(a)	$K \times K$	KM	$2K^2M + 2zKM(M-1) + 2yK^2M^2 + K^2M + (yKM)^2N$
Each fiber - EFR	Fig. 7(b)	$M \times zM$	-	$2zKM^2 + 2yK^2M^2 + K^2M + (yKM)^2N$
Each waveband - EBR	Fig. 7(c)	$K \times zK$	-	$2zK^2M + 2yK^2M^2 + K^2M + (yKM)^2N$

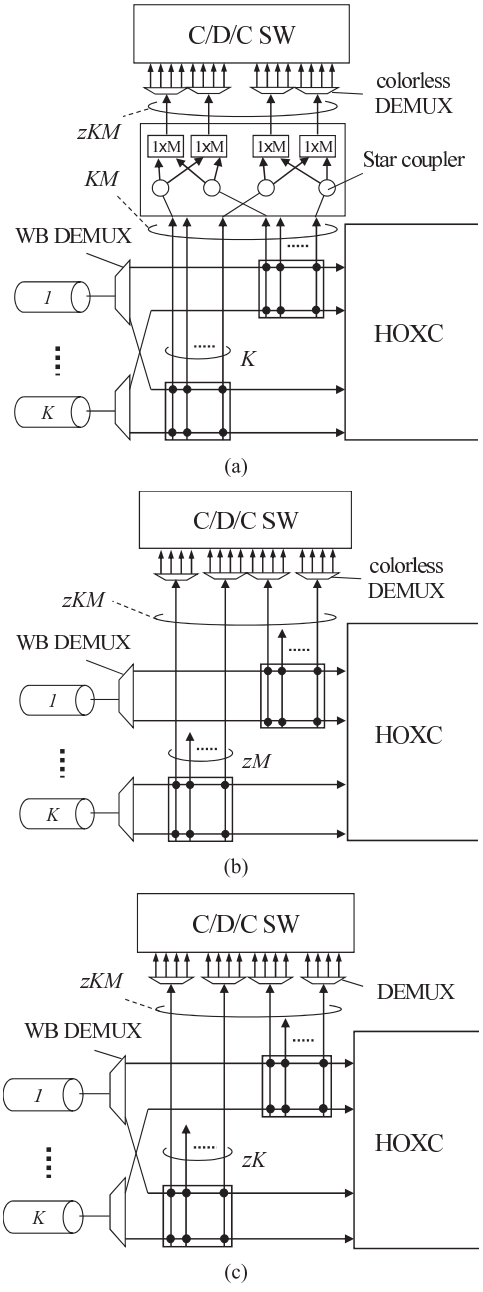

Fig. 7 Proposed HOXC architectures with restriction on waveband terminating ratio (only drop part is illustrated). (a) total restriction (TR). (b) each fiber restriction (EFR). (c) each waveband restriction (EBR).

signed matrix SWs for waveband grooming operation (see Fig. 2). Similar to the case of the single-layer OXC, it should be noted that the dedicated SW part of the proposed TR-HOXC is rearrangably non-blocking. In contrast, the dedicated SW part in the proposed EFR or EBR-HOXC provide strictly non-blocking operation. At the input port of the C/D/C SW, a dropped waveband path is demultiplexed to several wavelength paths. The C/D/C SW then rearranges those wavelength paths in any order. Therefore, the dedicated SW part selects the designated number of dropped or added waveband paths.

4. Numerical Evaluation and Comparison of HOXCs vs. Single-Layer OXC

The SW scale is evaluated by counting the number of cross-points including the drop side SW for termination as well as the add side SW for origination and the cross-connect part that is denoted as single-layer OXC and HOXC (see Figs. 6 and 7). This evaluation contains all the SWs except for C/D/C SWs because the necessary scale of the C/D/C SW is the same in both the single-layer OXC and the HOXC, if the originating/terminating ratio is the same. The number of cross-points is an exact discrete value when its component parameter is an integer (for example zK). For some cases, the parameter is not an integer, therefore, the SW scale can be approximated by interpolating with exact integer values.

4.1 Switch Scale Evaluation in Single-Layer OXC

We compare the SW scales of the proposed three single-layer OXCs and the conventional one shown in Fig. 1. Figure 8 shows SW sizes evaluated when the number of fibers, K, is changed, where the fiber capacity is assumed to be $L = 96$, and the originating/terminating ratio z is 0.375. It is found that the single-layer OXC with each wavelength restriction offers drastically reductions in SW scale compared to the other SWs with add/drop restriction. The proposed architecture exhibits small SW scale reduction compared to the conventional single-layer OXC by separating the add/drop functions and using dedicated SWs; both of them restrict the add/drop operation with each wavelength manner.

Figure 9 also plots the SW size variations in terms of z, where K and L are set at 8 and 96, respectively. This graph indicates a similar trend to that in Fig. 8, i.e., the proposed single-layer OXC with each wavelength restriction achieves minimum SW size for all originating/terminating ratios. The proposed EWR-SW exhibits a relatively smaller increase rate against an increase in the originating/terminating ratio compared to the TR or EFR architecture.

In Fig. 10, the switch scales of different single-layer OXC architectures are compared where L is variable. Other parameters, K and z, are set at 8 and 0.375 respectively. It is

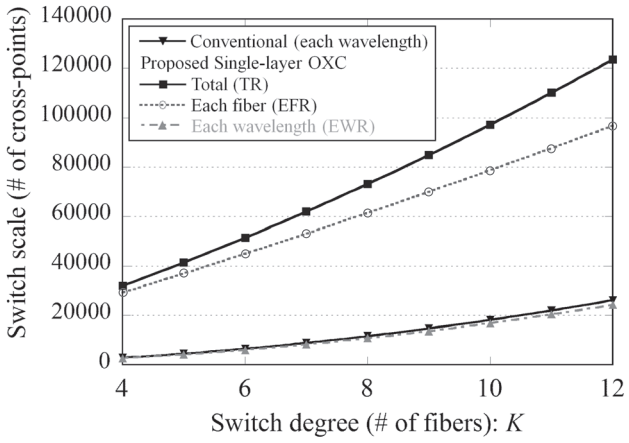

Fig. 8 Switch scale evaluation for different single-layer OXC architectures; switch degree K is variable. $L = 96$, $z = 0.375$.

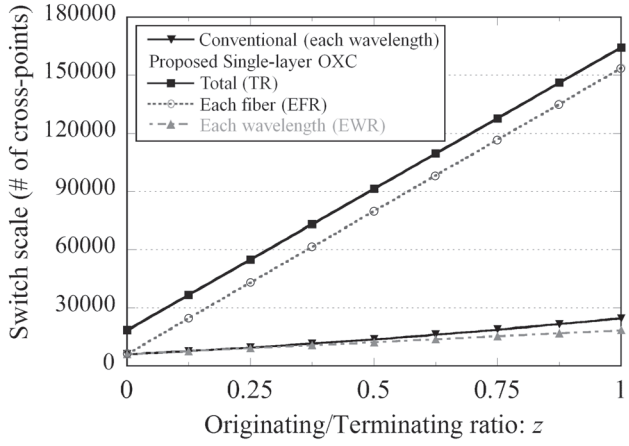

Fig. 9 Switch scale evaluation for different single-layer OXC architectures; originating/terminating ratio z is variable. $K = 8$, $L = 96$.

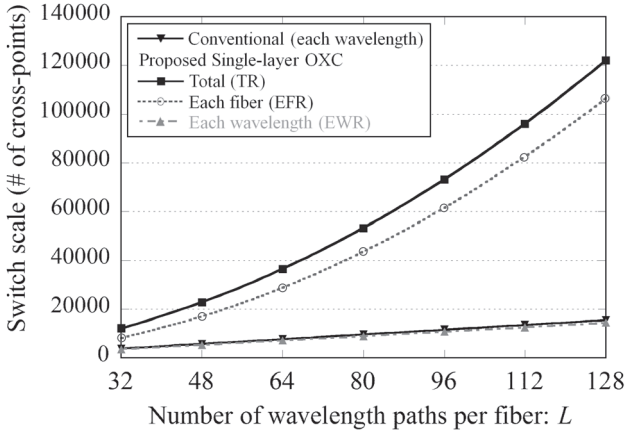

Fig. 10 Switch scale evaluation for different single-layer OXC architectures; number of wavelength paths per fiber L is variable. $K = 8$, $z = 0.375$.

difficult to reduce the scale of TR or EFR-SWs because their size is the square of L. The each wavelength restriction, dividing SWs into each wavelength index, can lower the order of SW size increase against the number of wavelength paths.

As shown in the above numerical examples, since hardware scale is much larger than that of the conventional single-layer OXC, especially TR and EFR single-layer OXCs, there is no advantage in terms of switch scale. However, an important point to be noted is that the three proposed single-layer OXC architectures have different ways of implementing originating/terminating operations. These differences directly affect the network dimension, that is, the necessary amount of network resources including fibers and cross-connect ports. In considering the network design problem, TR restriction offers the most relaxed constraint among the three restrictions. TR restriction is, therefore, favorable from the viewpoint of number of needed fibers, but it yields very large switch scale. In contrast, EWR restriction can achieve small switch scale, but it requires more fibers. We need to carefully choose the best solution considering the combination of switch cost and fiber cost [27], [28]. Looking at this issue from another perspective, only the EWR architecture has the same restriction with regard to the originating/terminating function as the conventional one. We can observe the effectiveness of our proposed idea, separation of add/drop operation, compared to the conventional architecture. It is verified since the proposed idea reduces the total switch scale. (This is seen more clearly in Fig. 12, which is explained later.)

4.2 Switch Scale Evaluation in HOXC Case and Comparison of HOXC vs. Single-Layer OXC

This subsection compares the SW scales of the three HOXC architectures and the single-layer OXCs. Two single-layer OXCs are considered; one is shown in Fig. 1, and the other is shown in Fig. 6(c). In this evaluation, the parameter of grooming ratio, y, is assumed to be 0.25. As mentioned before, the reason for choosing this value derives from the fact that the efficient algorithm in [20] yields almost the same performance at this value as when no grooming restriction is imposed.

Figure 11 shows the evaluated SW scale with regard to K, where the following parameters are used; $M = 8$, $N = 12$, thus $L = 96$, $z = 0.375$. The proposed HOXC architectures that use dedicated SWs for origination and termination greatly reduce SW size regardless of restriction type, unlike the conventional and proposed single-layer OXCs. The proposed TR architecture achieves over 37% SW scale reduction for all switch degrees. The proposed EFR and EBR architectures attain over 45% SW scale reduction. The proposed HOXCs with each waveband restriction and each fiber restriction offer almost the same SW scale.

Figure 12 shows the SW scale variation versus z when $K = 8$, $M = 8$, $N = 12$. It is clarified that the proposed HOXC architectures substantially reduce SW size compared to the single-layer OXCs regardless of restriction type. The result also shows that the proposed HOXC variants hold switch size almost constant as originating/terminating ratio z increases. It should be noted that the SW scale evaluations

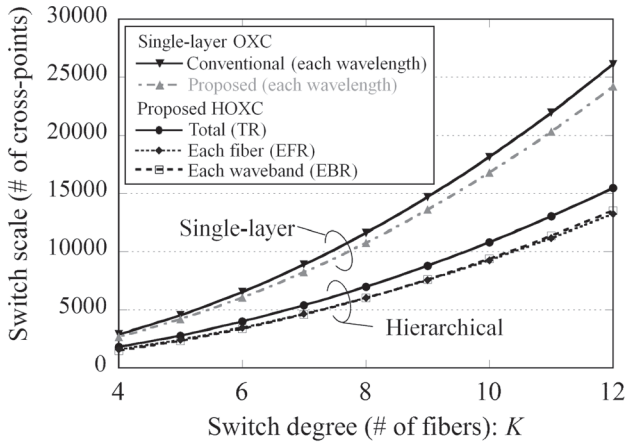

Fig. 11 Switch scale evaluation for different HOXC architectures; switch degree K is variable. $M = 8$, $N = 12$, $L = 96$, $z = 0.375$.

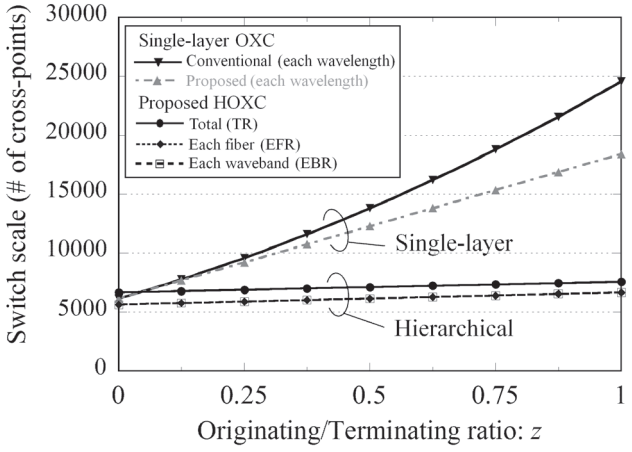

Fig. 12 Switch scale evaluation for different HOXC architectures; originating/terminating ratio z is variable. $K = 8$, $M = 8$, $N = 12$, $L = 96$.

in this paper do not include the C/D/C SW part (common to all switches). The scale of C/D/C SW increases in proportion to the square of the originating/terminating ratio. If the C/D/C switches are realized based on matrix switches, the number of cross-points is 82944 for the case of $K = 8$, $L = MN = 96$, $z = 0.375$. However, we can reduce the necessary number of cross-points significantly by applying 3-stage Clos network configuration [26]. Please note that, as mentioned in the Introduction, the C/D/C switch part can be realized with various technologies, including electrical switches and ODU cross-connects.

Figure 13 shows a SW scale comparison when the number of wavelength paths L is parameterized (note that the number of wavebands per fiber, M, is fixed to 8). Other parameters are as follows, $K = 8$, $z = 0.375$. Therefore, the number of wavelength paths per waveband increases with L. On the contrary to the single-layer OXC shown in Fig. 10, the TR and EFR architectures afford a linear increase in SW scale. This is because the waveband capacity becomes large as the number of wavelength paths per fiber increases.

As indicated in Figs. 11 to 13, owing to the coarse routing granularity offered by wavebands, an EFR-HOXC can decrease the number of required switch elements significantly. The EFR-HOXC greatly enhances switch scale reduction compared to the single-layer OXCs with the same constraint.

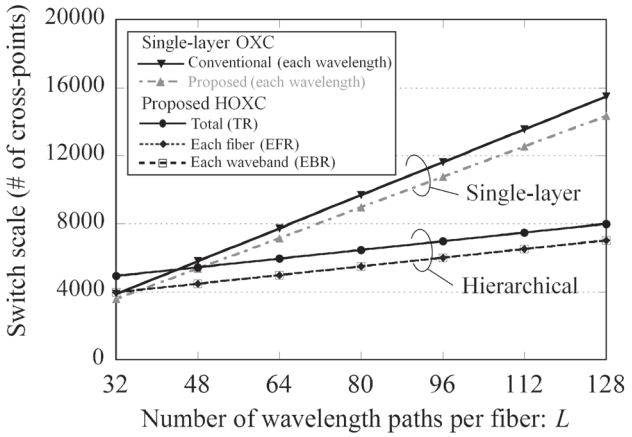

Fig. 13 Switch scale evaluation for different HOXC architectures; number of wavelength paths per fiber L is variable. $K = 8$, $M = 8$, $z = 0.375$.

5. Conclusion

This paper proposed novel optical node architectures that set constraints on the number of added/dropped optical signals. The proposed node architectures separately implement the add/drop functions for originating/terminating operations and grooming operations. The proposed HOXCs use dedicated switches for originating/terminating operations with different types of restrictions. For both single-layer OXC and HOXC, three types of restriction were presented. Numerical evaluations revealed that the proposed HOXC architectures can significantly reduce total switch scale. Moreover, implementation of dedicated switches for origination/termination enables the number of input ports of a switch that offers colorless, directionless and contentionless capability to be reduced, which reinforces the benefits of the proposed architectures.

Acknowledgments

This work was partly supported by NICT early-concept grants for exploratory research on new-generation network and JSPS KAKENHI (226957).

References

[1] K. Sato, "Recent developments in and challenges of photonic networking technologies," IEICE Trans. Commun., vol.E90-B, no.3, pp.454–467, March 2007.
[2] K. Sato, Advances in Transport Network Technologies: photonic networks, ATM, and SDH, Artech House, Norwood, MA, 1996. (ISBN 0-89006-851-8).
[3] ITU-R Recommendation, BT.1769, "Parameter values for an expanded hierarchy of LSDI image formats for production and international program exchange," Jan. 2006.

[4] G.K. Edwards, "Today's optical network research infrastructures for E-science applications," Proc. Opt. Fiber Commun. Conf. National Fiber Optic Eng. Conf., Paper OWU3, March 2006.
[5] K. Sato and H. Hasegawa, "Optical networking technologies that will create future bandwidth-abundant networks," OSA/IEEE J. Opt. Commun. Netw., vol.1, no.2, pp.A81–A93, July 2009.
[6] K. Sato and H. Hasegawa, "Prospects and challenges of Multi-layer optical networks," IEICE Trans. Commun., vol.E90-B, no.8, pp.1890–1902, Aug. 2007.
[7] X. Cao, V. Anand, and C. Qiao, "Framework for waveband switching in multigranular optical networks: Part I — Multigranular cross-connect architectures," OSA J. Opt. Netw., vol.5, no.12, pp.1043–1055, Dec. 2006.
[8] K. Harada, K. Shimizu, T. Kudou, and T. Ozeki, "Hierarchical optical path cross-connect systems for large scale WDM networks," Proc. Opt. Fiber Commun. Conf. National Fiber Optic Eng. Conf., pp.356–358, Feb. 1999.
[9] L. Noirie, C. Blaizot, and E. Dotaro, "Multi-granularity optical cross-connect," Proc. Eur. Conf. Opt. Commun., pp.269–270, Oct. 2000.
[10] P. Torab, V. Hutcheon, D. Walters, and A. Battou, "Waveband switching efficiency in WDM networks: Analysis and case study," Proc. Opt. Fiber Commun. Conf. National Fiber Optic Eng. Conf., Paper OTuG3, March 2006.
[11] X. Cao, V. Anand, Y. Xiong, and C. Qiao, "A study of waveband switching with multilayer multigranular optical cross-connects," IEEE J. Sel. Areas Commun., vol.21, no.7, pp.1081–1094, Sept. 2003.
[12] I. Yagyu, H. Hasegawa, and K. Sato, "An efficient hierarchical optical path network design algorithm based on a traffic demand expression in a Cartesian product space," IEEE J. Sel. Areas Commun., vol.26, no.6, Part Supp., pp.22–31, Aug. 2008.
[13] Y. Yamada, H. Hasegawa, and K. Sato, "Hierarchical optical path network design algorithm considering waveband protection," J. Lightwave Technol., vol.27, no.24, pp.5736–5748, Dec. 2009.
[14] Y. Yamada, H. Hasegawa, and K. Sato, "Survivable hierarchical optical path networks employing waveband and wavelength path protection," Proc. Opt. Fiber Commun. Conf. National Fiber Optic Eng. Conf., Paper OWY3, March 2009.
[15] H.-C. Le, H. Hasegawa, and K. Sato, "Hierarchical optical path network design algorithm considering waveband add/drop ratio constraint," OSA/IEEE J. Opt. Commun. Netw., vol.2, no.10, pp.872–882, Oct. 2010.
[16] S. Kakehashi, H. Hasegawa, and K. Sato, "Optical cross-connect switch architectures for hierarchical optical path networks," IEICE Trans. Commun., vol.E91-B, no.10, pp.3174–3184, Oct. 2008.
[17] R. Hirako, K. Ishii, H. Hasegawa, and K. Sato, "Compact matrix-switch-based hierarchical optical path cross-connect with colorless waveband add/drop ratio restriction," IEICE Trans. Commun., vol.E94-B, no.4, pp.918–927, April 2011.
[18] S. Mitsui, H. Hasegawa, and K. Sato, "Low loss and cost-effective hierarchical optical path cross-connect switch architecture based on WSS/WBSS," Proc. Photon. Switching, Paper FrII2-3, Sept. 2009.
[19] K. Ishii, H. Hasegawa, K. Sato, M. Okuno, and H. Takahashi, "Ultra-compact waveband cross-connect module using waveband selective switches: Development and performance verification," IEEE Photonics Technol. Lett., vol.22, no.23, pp.1741–1743, Dec. 2010.
[20] Y. Yamada, H. Hasegawa, and K. Sato, "Coarse granular routing in optical networks and impact of supplemental intermediate grooming," Proc. Eur. Conf. Opt. Commun., Paper Th.10.F.1, Sept. 2010.
[21] V. Kaman, R.J. Helkey, and J.E. Bowers, "Multi-degree ROADM's with agile add-drop access," Proc. Photon. Switching, Paper TuA2.5, Aug. 2007.
[22] K. Mizutani, M. Sakauchi, and A. Tajima, "Demonstration of multi-degree color/direction-independent waveguide-based transponder-aggregator for flexible optical path networks," Proc. Eur. Conf. Opt. Commun., Paper P3.11, Sept. 2010.
[23] S. Woodward, M. Feuer, P. Palacharla, X. Wang, I. Kim, and D. Bihon, "Intra-node contention in a dynamic, colorless, non-directional ROADM," Proc. Opt. Fiber Commun. Conf. National Fiber Optic Eng. Conf., Paper PDPC8, March 2010.
[24] R. Jensen, A. Lord, and N. Parsons, "Colourless, directionless, contentionless ROADM architecture using low-loss optical matrix switches," Proc. Eur. Conf. Opt. Commun., Paper Mo.2.D.2, Sept. 2010.
[25] R. Hirako, K. Ishii, H. Hasegawa, K. Sato, H. Takahashi, and M. Okuno, "Flexible and compact hierarchical optical cross-connect node with waveband add/drop restriction," Proc. Opt. Fiber Commun. Conf. National Fiber Optic Eng. Conf., Paper OTuE5, March 2011.
[26] T.S. El-Bawab, Optical Switching, Springer, 2006, ISBN 0-387-26141-9.
[27] F. Naruse, Y. Yamada, H. Hasegawa, and K. Sato, "Optical network design algorithms that consider add/drop ratio restrictions for OXC hardware scale reduction," Proc. Opt. Fiber Commun. Conf. National Fiber Optic Eng. Conf., Paper NThC3, March 2011.
[28] F. Naruse, Y. Yamada, H. Hasegawa, and K. Sato, "Evaluations of different optical path add/drop ratio restriction schemes on OXC hardware scale and network resource requirement," submitted to elsewhere.

Yoshiyuki Yamada received the B.E. and M.E. degrees in Electrical Engineering and Computer Science from Nagoya University, Nagoya, Japan, in 2007 and 2009, respectively. He is currently a graduate student of the Department of Electrical Engineering and Computer Science, Nagoya University. His major interests include optical network design and optimization, network survivability, and photonic node architecture. He is a member of IEEE.

Hiroshi Hasegawa received the B.E., M.E., and D.E. degrees all in Electrical and Electronic Engineering from the Tokyo Institute of Technology, Tokyo, Japan, in 1995, 1997, and 2000, respectively. From 2000 to 2005, he was an assistant professor of the Department of Communications and Integrated Systems, Tokyo Institute of Technology. Currently he is an associate professor of Nagoya University. His current research interests include Photonic Networks, Image Processing (especially Super-resolution), Multidimensional Digital Signal Processing and Time-Frequency Analysis. He received the Young Researcher Awards from SITA (Society of Information Theory and its Applications) and IEICE (Institute of Electronics, Information and Communication Engineers) in 2003 and 2005, respectively. Dr. Hasegawa is a member of SITA and IEEE.

Ken-ichi Sato received the B.S., M.S., and Ph.D. degrees in Electronics Engineering from the University of Tokyo, in 1976, 1978, and 1986, respectively. He is currently a professor at the Graduate School of Engineering, Nagoya University, and he is an NTT R & D Fellow. Before joining the university in April 2004, he was an executive manager of the Photonic Transport Network Laboratory at NTT. His R & D activities cover future transport network architectures, network design, OA&M (operation administration and maintenance) systems, photonic network systems including optical crossconnect/ADM and photonic IP routers, and optical transmission technologies. He has authored/co-authored more than 200 research publications in international journals and conferences. He holds 35 granted patents and more than 100 pending patents. He received the Young Engineer Award in 1984, the Excellent Paper Award in 1991, and the Achievement Award in 2000 from the Institute of Electronics, Information and Communication Engineers (IEICE) of Japan, and the Best Paper Awards in 2007 and 2008 from IEICE Communications Society. He was also the recipient of the distinguished achievement Award of the Ministry of Education, Science and Culture in 2002. His contributions to asynchronous transfer mode (ATM) and optical network technology development extend to co-editing the *IEEE Journal on Selected Areas in Communications* (three special issues) and the *IEEE Journal on Lightwave Technology* (special issue), organizing several workshops and conference technical sessions, serving on numerous committees of international conferences including OFC and ECOC, authoring a book, *Advances in Transport Network Technologies* (Artech House, 1996), and co-authoring thirteen other books. He is a Fellow of the IEEE.